Utami dkk. (2024) Vol. 12 No. 3: 221-232

Chimica et Natura Acta

p-ISSN: 2355-0864 e-ISSN: 2541-2574

Homepage: http://jurnal.unpad.ac.id/jcena

Development of Photo Electrocatalytic Chemical Oxygen Demand Design (PECOD) Sensor using Highly Ordered Titanium Dioxide Nanotube Arrays Electrodes

Chichi Amne Utami, Muhammad Iqbal Syauqi, Sherly Kasuma Warda Ningsih, Rahmat Wibowo, Jarnuzi Gunlazuardi*

Department of Chemistry, Faculty of Mathematics and Natural Science (FMIPA), Universitas Indonesia
Jl. Lingkar, Pondok Cina, Kecamatan Beji, Kota Depok, Jawa Barat 16424, Indonesia.
*Corresponding author: jarnuzi@ui.ac.id

DOI: https://doi.org/10.24198/cna.v12.n3.49333

Abstract: Population growth, industrialization, and the need to ensure water quality have fostered the demand for analytical methods and tools to determine one of the important values of water quality standards. The oxygen demand of a given water matrix provides valuable information about the presence of organic compounds in a sample. The TiO_2-based photoelectrocatalytic COD (PECOD) method offers a faster, more efficient, and more accurate alternative than conventional methods. Highly ordered TiO_2 nanotube arrays (HOTNAs) were synthesized by anodizing titanium metal at 45V for 2 hours. HOTNAs/FTO photoanodes are used to oxidize organic compounds in water. HOTNAs/FTO photoanode has a bandgap of 3.4eV and a current density of 0.29 mA/cm^2. Environmental samples were tested with the PeCOD sensor using glucose and mixed compound addition standards method. Water samples taken from local small ponds, namely Danau Kenanga, Danau Agathis, and typical wastewater of Laundry activity reveal COD values of 15,4659 to 15,9571 mg/L O_2; 19,0500 to 19,6179 mg/LO_2; 445,2336 to 449,7830 mg/L O_2; respectively. The developed PECOD sensor performed well and provided analytical results that were not much different from conventional methods, with an error percentage below 10%.

Keywords: highly ordered TiO_2 nanotube arrays (HOTNAs), photoelectrocatalysis, chemical oxygen demand.

Abstrak**:** *Pertumbuhan populasi, industrialisasi, dan kebutuhan untuk memastikan keamanan air mendorong permintaan metode dan perangkat analisa untuk mengetahui salah satu nilai penting baku mutu air. Kebutuhan oksigen dari matriks air tertentu memberikan informasi penting tentang keberadaan senyawa organik dalam sampel. Metode pengukuran kebutuhan oksigen kimiawi secara fotoelektrokimia (Photoelectrokatalitik Chemical Oxigen Demand, PECOD) berbasis TiO_2 menawarkan alternatif yang lebih cepat, lebih efisien, dan lebih akurat dibandingkan metode konvensional. Sintesis Highly Ordered TiO_2 Nanotube Arrays (HOTNAs) dilakukan dengan metode anodisasi pada 45V selama 2 jam. Fotoanoda HOTNAs/FTO digunakan untuk mengoksidasi senyawa organik dalam air. Fotoanoda HOTNAs/FTO memiliki celah pita sebesar 3,4eV dan densitas arus 0,29 mA/cm^2. Sampel lingkungan yang telah diuji dengan sensor PeCOD menggunakan standar adisi glukosa dan senyawa campuran yaitu air permukaan Danau Kenanga menghasilkan COD sebesar 15,4659 mg/L $O_{2;}$ dan 15,9571 mg/L $O_{2.}$, air permukaan Danau Agathisa menghasilkan COD sebesar 19,05 mg/L O_2 dan 19,6179 mg/L O_2, dan sampel Laundry-X menghasilkan COD sebesar 445,2336 mg/L O_2 dan 449,783 mg/L O_2. Sensor PECOD yang dikembangkan menunjukkan kinerja yang baik, liniearitas, sensitifitas, dan mampu memberikan hasil analisa yang tidak berbeda jauh dibandingkan dengan metoda konvensional dengan %kesalahan dibawah 10%.*

Kata kunci: *highly ordered* TiO_2 *nanotube arrays (HOTNAs), fotoelektrokatalisis, PECOD, sensor kualitas air,* TiO_2

INTRODUCTION

Water is an essential part of the ecosystem for life on Earth (Singh *et al*. 2023). However, with rapid population growth and socio-economic development, the use and scarcity of this limited surface fresh water is increasing rapidly. According to statistics, a quarter of the world's population does not have access to clean water, and half of the world's population does not have access to proper sanitation. Therefore, continuous monitoring and quality control of surface fresh water in all world countries is a priority (Syeed *et al*. 2023).

Water quality testing is the first step in controlling water pollution. Chemical Oxygen Demand (COD) of water and wastewater is one of the most important parameters for measuring water quality. Given the inherent disadvantages of standard dichromate methods, such as the process which takes 2-4 hours, generates highly toxic ions (Cr^{6+} and Hg^{2+}), applies corrosive reagents (concentrated H_2SO_4), and is expensive (Ag_2SO_4), much has been invested in the development of new, faster, and more environmentally friendly methods for determining COD (Si *et al*. 2019). In recent years, the development of new, faster, and more environmentally friendly methods for determining COD has been reported (Cazaudehore *et al*. 2019). The photo electrocatalysis (PEC) method can achieve the best solution, which uses a semiconductor material as a photoelectrode. This photoelectrode allows electrons to be excited from the valence band (VB) to the conduction band (CB) in light radiation with superband gap energy, producing strong oxidizing species (Chen *et al*. 2022).

The principle of PEC technology improvement is developing photoelectrodes and designing PEC cells for high-efficiency and simple processes. PEC-based COD sensor (PeCOD) technology has been applied in various industries, such as industrial and urban wastewater, drinking water, food, and paper (Azer *et al*., 2022). PeCOD technology has the potential to be a superior COD measurement method compared to traditional methods. However, the PeCOD sensor has several weaknesses. It is relatively complicated to make, has high testing costs, and still needs to be widely available in the market. The photoelectrode development strategy involves selecting and developing suitable semiconductors and their support electrodes (Kangkun & Ponchio 2020).

TiO_2 is an n-type semiconductor with a wide bandgap energy (Garcia-Segura & Brillas 2017). When UV light irradiates TiO_2, it provides an electron-hole pair, eventually producing strong oxidizing species on its surface. TiO_2 semiconductors are used in many fields due to their high oxidation properties, non-toxicity, environmental safety, good chemical stability, and corrosion resistance (Syauqi *et al*. 2023).

Highly ordered TiO_2 nanotube arrays (HOTNAs) are a good choice for photoelectrochemical (PEC) applications because the HOTNAs have good structural stability, a small volume that allows efficient charge transport, and a high specific surface area and surface area for light absorption (Cao *et al*. 2021). TiO_2 nanotubes have been prepared using various techniques such as hydrothermal (Yu *et al*. 2006), electrospinning (He *et al*. 2013), and electrochemical anodization (Syauqi *et al*. 2023). Electrochemical anodization has several advantages, namely a simple and inexpensive process (Fu & Mo 2018), can produce nanotubes with the desired morphology (Puga *et al*. 2022), high photocatalytic activity, corrosion resistance, and bioactivity (Nogueira *et al*. 2021), and produces nanotube arrangements aligned with temperature annealing (Abbas *et al*. 2019), potential, anodizing time, type of electrolyte and pH value that can affect the growth process of TiO_2 nanotubes (Azer *et al*. 2022).

This study aims to develop a photoanode employing HOTNAs film coated onto fluor-doped tin oxide (FTO) substrates for use as photo-electrocatalytic chemical oxygen demand (PECOD) sensors. We have also developed a PECOD cell design that is simple, economical, convenient, and highly efficient in COD measurement. Most importantly, the developed PECOD cell effectively determines COD values with a simple, fast, and environmentally friendly method, making it suitable for further development in water pollution monitoring.

MATERIALS AND METHODS

Materials.

Titanium (Ti) foil (99.6% purity, 0.3 mm thickness) was purchased from Sigma Aldrich, 1500 cc and 2000 cc abrasive paper, TiO_2 Evonic P25, stainless steel foil acetone, ethanol, deionized water, NH_4F (0.3% w), ethylene glycol, glucose, oxalic acid, KHP, benzoic acid, were obtained from Merck; environmental samples were collected from local water surface.

Preparation of Highly Ordered TiO_2 Nanotube Arrays (HOTNas)/Ti.

HOTNAs are made by the anodizing method. Before anodizing, Ti plates with a length and width of 1.5x4.0 cm and thickness of 0.2 mm were cleaned using 1500 cc and 2000 cc abrasive paper. After that, the plates were sonicated in acetone, ethanol, and distilled water for 10 minutes each, then dried in air. The cleaned Ti plate was then dipped into the reactor filled with electrolyte solution consisting of ethylene glycol solution containing 2% v/v distilled water 0.3% w/w NH_4F. The anodization process was carried out by placing a Ti plate as the anode and a stainless-steel plate as the cathode, with the electrode spacing set at 1.5 cm. The anodization process was carried out using a DC power supply with 45 V at two electrodes for 2 hours. The current and time during the anodizing process are recorded. After anodizing, the samples were soaked in ethanol for 20 minutes and air-dried, then the Ti plate was annealed at 450°C for 2 hours with a heating rate of 2°C/min. From this process, anatase HOTNAs will be obtained.

Detachment process of HOTNAs film from Ti plate.

To detach the HOTNAs film from the Ti Plate, the Ti plate was re-anodized at a constant voltage of 30 V DC for 20 minutes using the same electrolyte. Furthermore, the re-anodized samples were immersed in a 30% H_2O_2 solution for a few minutes until the film turned light yellow, and then the samples were soaked in ethanol. After that, the plate was dried in the air, and the HOTNAs film detached itself from the Ti substrate.

Transplantation process of HOTNAs film onto Fluor Doped Tin Oxide (FTO) substrate.

The HOTNAs film that has been detached from the Ti substrate is transplanted onto the FTO substrate by placing TiO_2 suspension between the HOTNAs film and the FTO substrate. TiO_2 adhesive was prepared by dissolving 0.02 g of Degusssa TiO_2 powder with 2 mL of ethanol. Three drops of TiO_2 suspension were dripped onto the FTO substrate as an adhesive between the HOTNAs film and the FTO substrate.

Synthesis of Pt/FTO.

The Pt/FTO electrodes were prepared by cleaning the FTO glass using sonication in acetone, ethanol, and distilled water for 30 minutes, respectively. The Pt/FTO conductive surface was prepared by dropping 40 mM $H_2PtCl_{6,}$ followed by calcination at 380°C for 30 minutes.

The preparation of HOTNAs/FTO includes several major steps. Figure 1 illustrates the overall HOTNAs/FTO preparation process, which begins with the anodization of Ti plates to produce HOTNAs/Ti. This is followed by a detachment process to obtain the HOTNAs film, which is subsequently transplanted onto FTO glass substrates. Finally, the assembly of these components results in the formation of a complete sensor cell.

Characterization of HOTNAs/FTO films.

The HOTNAs film was characterized using a Fourier-transformed infra-red instrument (Ir Prestige-21, Shimadzu, Japan). The crystallinity phases of the HOTNAs/Ti and HOTNAs/FTO films were investigated using X-ray diffraction with CuKα irradiation at λ 1.54 Å (Malvern Panalytical, UK). The morphology of the films was analyzed using a Field Emission Scanning Electron Microscope (FE-SEM) equipped with X-ray energy spectroscopy (EDS). The diffuse reflectance spectra of HOTNAs/FTOs were recorded using a UV-Vis diffuse reflectance spectrophotometer (UV-2450 Shimadzu, Japan).

Photoelectrochemical properties were analyzed by Linear sweep voltammetry (LSV) at 25 mV/s scan rate from -1V to +1V and Multipulse Amperometry (MPA) technique at 0 V vs Ag/AgCl in 0.1 M $NaNO_3$ solution. The HOTNAs film, Pt/FTO, and Ag/AgCL were used as working, counter, and reference electrodes, respectively. A 13-watt UV lamp and a 15-watt visible light lamp were used as illumination sources.

Fabrication of PECOD Probe Reactor with Flow Injection Analysis System.

The PECOD sensor cell is created with a flow injection system design. Figure 2a is the design of the COD probe. The flow system probe reactor was constructed using acrylic material with a length of 8 cm, a width of 4 cm, and a height of 2.5 cm. The sensor cell has a volume of 1 cm^3. The COD probe comprises two electrodes: HOTNAs/FTO as the working electrode and Pt/FTO as the counter electrode. Figure 2b is a schematic of the flow injection analysis reactor system. The reactor was made of wood covered with aluminum foil. In finalization, one piece of UV lamp and one piece of Vis lamp were inserted.

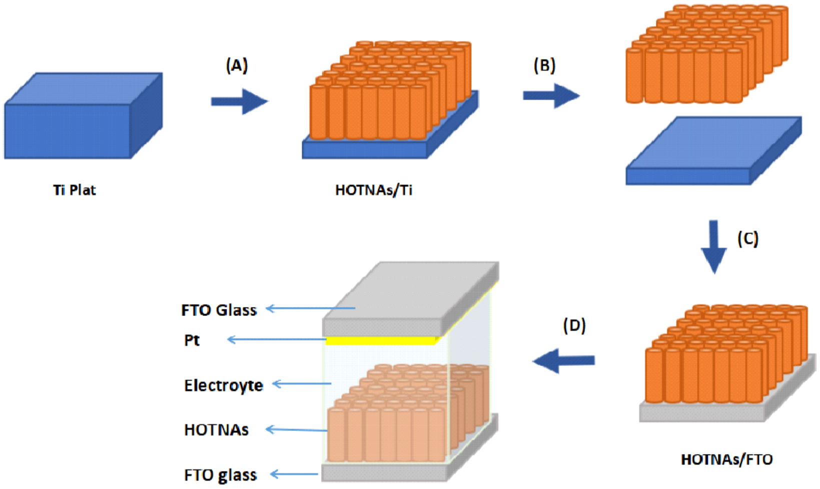

Figure 1. Schematic of the whole HOTNAs/FTO preparation process (a) Anodizing Ti plate, (b) Detachment process of HOTNAs film from Ti plate, (c) Transplantation process of HOTNAs film on the FTO glass (d) Fabrication of the sensor cell.

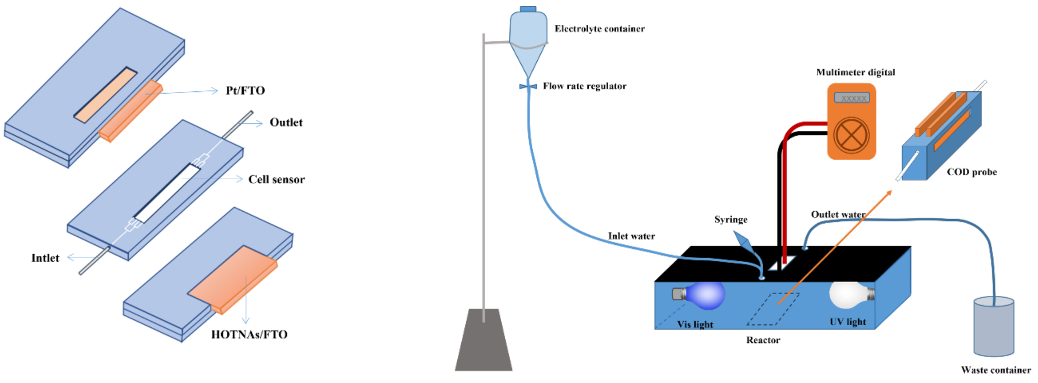

(a) (b)

Figure 2. (a) The design of COD probe, (b) The scheme of flow injection analysis system reactor

COD Calculation.

During photo electrocatalysis, a photocurrent from clean water containing electrolytes as the blank (i_{blank}) represents the current obtained from water without any organic chemical content. In comparison, the photocurrent produced from a solution containing organic chemicals (i_{tot}) is current from the oxidation of organic compounds in water. So, the net photocurrent (i_{net}) is (Zhao *et al*. 2004):

$i_{net} = i_{tot} – i_{blanko}$ … (1)

According to Faraday's law, the net charge (Q_{net}) resulting from the reaction is as follows (Zhao *et al*. 2004):

$$\int idt = nFVC \text{ ... (2)}$$

The strong oxidizing ability of the photo-generated holes on the TiO_2 photoelectrode resulting in the photocatalytic oxidation of organic compounds through the TiO_2 electrode will produce an oxidation reaction stoichiometry of (Zhang *et al*. 2004):

$C_yH_mO_jN_kX_q + (2y−j)\ H_2O \rightarrow yCO_2 + qX^- + kNH_3 + (4y−2j + m−3k)\ H^+ + (4y−2j + m−2k−q)\ e^-$ … (3)

Thus, the number of electrons transferred becomes (Zhao *et al*. 2004):

$n = 4y − 2h + m − 3k – q$ … (4)

Thus, the net charge, according to Faraday's law becomes (Zhang *et al*. 2004):

$Q = nFVC = (4y−2h+m−3k–q)\ FVC= kC$ … (5)

This is because one molecule of oxygen is equivalent to the electrons transferred in the reduction reaction of oxygen Zhao *et al*. 2004):

$O_2 + 4H^+ + 4e^- \rightarrow 2H_2O$ … (6)

Then, the Q value can be used to calculate the COD value (in terms of mg/L O_2) according to the following equation Zhao *et al*. 2004):

$[COD]\ (mg/L\ O_2) = Q/4FV \times 32000$ … (7)

Where F is the Faraday constant and V is the actual volume of photoanode occupied by the organic compound. For any given probe design, the V values can be determined by experiment, as an experimental constant.

RESULT AND DISCUSSION

Preparation of HOTNAs/Ti.

The current generated during the anodization process (45 V, 2 hrs) was recorded and analyzed. In Figure 3, three stages of current changes are observed during anodization. In stage 1, the current has decreased sharply, indicating the formation of a white layer of TiO_2 (equations 8 and 9). The formation of TiO_2 film resulting the electron transfer rate between the titanium metal and the electrolyte becoming obstructed, which can be seen from the decrease in current. In stage 2, the current profile increased due to an increase in anode conductivity due to the formation of small holes due to the dissolution of TiO_2 by F^- ions to form a $[TiF_6]^{2-}$ complex (equation 10). In stage 3, a decrease in current is shown, followed by a steady state profile, which shows an equilibrium reaction between TiO_2 dissolution and TiO_2 formation. The reactions that occur could be considered as follows:

$Ti \rightarrow Ti_4^+ + 4e^-$ … (8)
$Ti_4^+ + 2H_2O \rightarrow TiO_2 + 4H^+$ … (9)
$TiO_2 + 6F^- + 4H^+ \rightarrow [TiF_6]_2^- + 2H_2O$ … (10)

Figure 4a shows a picture image of the Ti plate before anodizing. The Ti plate before anodizing is a bright silver color, and then after anodizing, the Ti plate turns blueish due to oxide growth, as shown in Figure 4b. This is a thin layer of HOTNAs on top of a titanium substrate. The detachment process of HOTNAs film is carried out as soon as possible after the second anodization process is completed because if it is not carried out immediately, the film when lifted, will interact with air which makes the HOTNAs film bond with the Ti substrate stronger and will be difficult to detach. The resulting HOTNAs films are white (shown in Figure 4c). In Figure 4d, the HOTNAs film was transplanted onto the FTO with a few drops of TiO_2 suspension using the doctor blade method.

Characterization of synthesized HOTNAs/FTO photoelectrodes.

The results of HOTNAs/Ti and HOTNAs/FTO characterization are shown in Figure 5. Figure 5a shows the FTIR spectra of the Ti plat, HOTNAs/Ti, and HOTNAs/FTO. The HOTNAs/Ti and HOTNAs/FTO spectra show a pattern almost similar to the absorption characteristics of Ti-O-Ti at wavenumbers 480-1200 cm^{-1}. OH-bending and OH-stretching were also seen at 1500-1650 cm^{-1} and 3500-3000 cm^{-1}, respectively. This result is consistent with the literature, which shows that the Ti-O-Ti bond is observed at wave number 483 cm^{-1} (Chougala *et al*. 2017).

The XRD diffraction pattern of HOTNAs/Ti and HOTNAs/FTO can be seen in Figure 5b. Based on COD data no. 96-900-9087 and COD data 96-901-6191, sample HOTNAs/Ti showed typical peaks of anatase and Titanium. The HOTNAs/FTO sample based on COD data no. 96-900-9087 shows a typical peak of anatase.

These results concluded that transplanting HOTNAs films to FTO did not change the crystal structure. The size of the crystallites formed was calculated using the Debye-Scherer equation (Alkorbi *et al*. 2022), resulting in an average crystal size of HOTNAs/Ti and HOTNAs/FTO of 38.96 nm and 40.07 nm, respectively.

The top and cross-section morphology of HOTNAs/Ti and HOTNAs/FTO are shown in Figure 6. In Figure 6 a, HOTNAs/Ti shows a cylindrical structure with a uniform pore diameter of 38.61 nm and regularly arranged walls with a tube height of 9.029 µm. This structure consists of a series of hollow tubes aligned repeatedly, creating a large surface area and a conductive pathway for electrochemical reactions (Ocampo *et al*. 2023; Li *et al*. 2008; Tesler *et al*. 2020). While in Figure 6b, the HOTNAs film transplanted on FTO glass shows a change in the TiO_2 structure from nanotubes to deformed nanotubes. Under these conditions, the TiO_2 structure showed more pores and irregular walls with a tube wall height of 1.35 µm. This structural

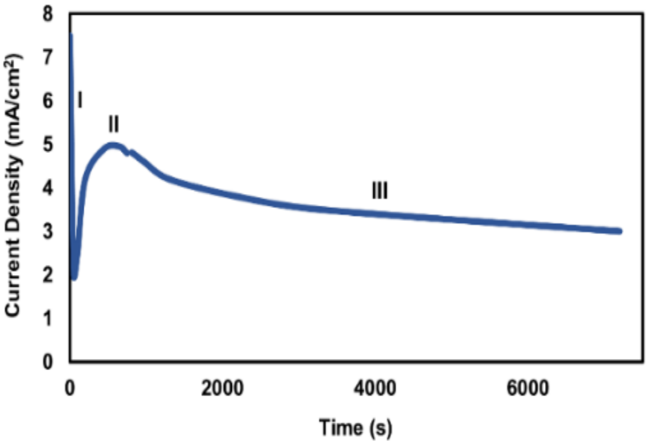

Figure 3. Anodizing current density curve Vs. time

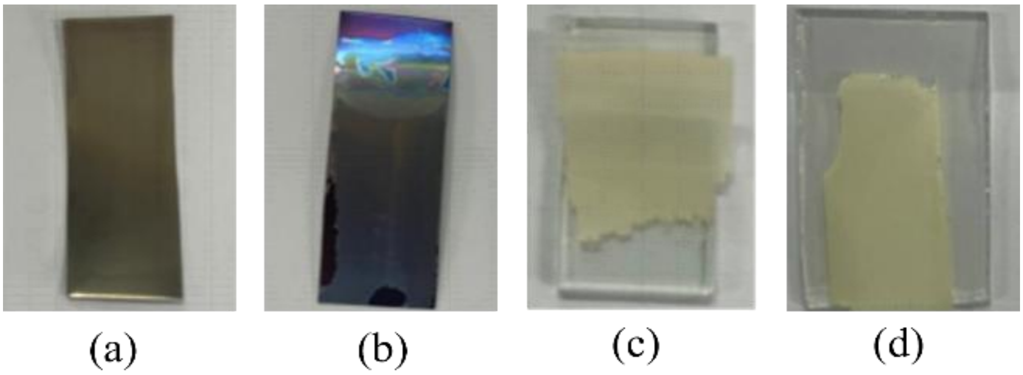

Figure 4. Ti plate (a) before anodizing, (b) after anodizing 45 V 2 for 2 hours, (c) peeling off the HOTNAs film, and (d) bonding the HOTNAs film on the surface of the FTO substrate.

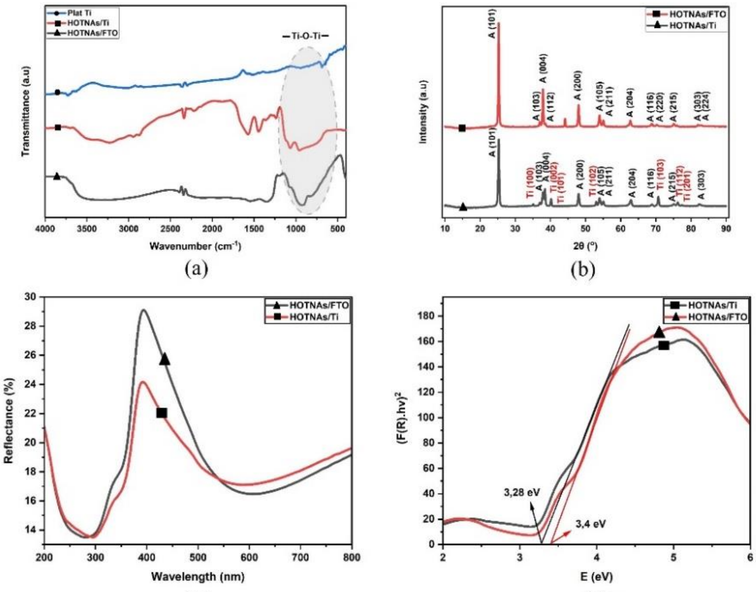

(a) (b)

(c) (d)

Figure 5. Characterization of HOTNAs/Ti and HOTNAs/FTO syntheses (a) FTIR spectra, (b) X-Ray Diffractograms, (c) UV-Vis DRS spectra, (d) Tauc Plot for Band

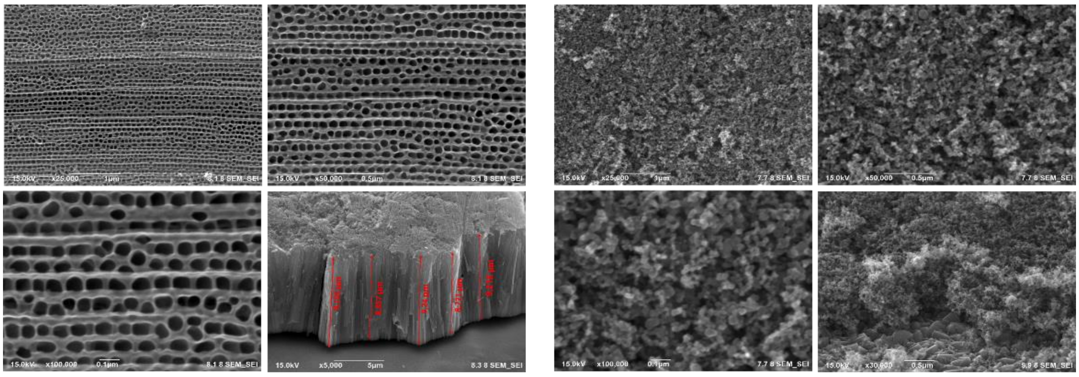

(a) (b)

Figure 6. FESEM image a) HOTNAs/Ti, b) HOTNAs/FTO

change can be influenced by synthesis conditions, such as the release process and the HOTNAs film transplantation process to FTO (Yang *et al*. 2016).

The HOTNAs films peeled from the Ti substrate were transplanted into FTO using the blade doctor method. The photocatalytic response was examined by Linear Sweep Voltammetry (LSV) and Multi Pulse Amperometry (MPA) under different conditions, irradiated with ultraviolet (UV) light and visible (Vis) light. Figure 7 compares HOTNAs/Ti and HOTNAs/FTO electrodes. HOTNAs/FTO produces a better current density than HOTNAs/Ti, possibly because the typical HOTNAs/FTO peak is dominated by anatase and has a higher crystallite size than HOTNAs/Ti (Misriyani *et al*. 2015; Zerjav *et al*. 2022).

COD Probe Reactor Flow Injection Analysis System.

Photos of the main components of the COD sensor device using a flow system are shown in Figure 8. Figure 8(a) shows a COD sensor probe made with acrylic material with a length of 8 cm, a width of 2 cm, and a height of 4 cm. The COD sensor probe has two electrodes: Pt/FTO and HOTNAs/FTO. The inside of the sensor cell, where the electrodes, electrolytes, and analytes are made with a volume of 1 cm^3 with a distance of 0.5 cm for the Pt/FTO and HOTNAs/FTO electrodes. The surface area of the electrode on the sensor cell is 2 cm^2. The probe has inlet and outlet holes with an inside diameter of 1 mm. An illustration of the COD sensor probe can be seen in Figure 2 (a). Resin and hardener gaskets are provided at the inlet and outlet to close the channels connected to other devices to avoid liquid leakage. The COD probe consists of three layers of acrylic, as shown in Figure 2(a), with each layer given silicone rubber as a liaison and prevents leakage during testing.

Figure 8(b) shows the overall arrangement of the FIA system. The internal structure of the wooden reactor can be seen in Figure 2b. there are two lamps: one UV lamp and one Vis lamp. The UV lamp was used as a photon energy source to activate TiO_2 photocatalysis for COD oxidation. The FIA system in this study relies on gravity flow and uses a commercial infusion tube with an inner diameter of 2.5 mm. The gravity flow method uses the force of gravity to push the sample flow through the system. This method is relatively simple as it does not require a pump or other high-pressure device. The sample flow can be controlled in a controlled manner without the need for complex resources by adjusting the height and slope of the system. This makes the gravity flow method efficient and inexpensive for PECOD measurements with a flow system.

Figure 8b shows that the electrolyte is placed in a container with a height and tilt that has been set. The 0.1 M $NaNO_3$ electrolyte flowed from an infusion tube, and various water samples were injected using a syringe. Typically, 0.05 mL of the sample was injected and then flowed into the PECOD probe with a sensor cell volume of 1 cm^3. The organic compounds in the water sample that reach the photoanode will be oxidized, and a commercial digital multimeter will measure the photocurrent response. Due to the large cell space factor with the flow using the gravity method, the flow rate is set to 0.1333 mL/s so that the retention time of the sample solution in the sensor cell is 7.5 seconds. With a speed of 0.1333 mL/s, it provides good contact conditions between samples in the sensor and is sufficient to accommodate photoelectrochemical oxidation reactions efficiently. The plot between the Q value and the variation in concentration (Figure 9) shows a high and linear Q value with increasing concentration. A high Q value indicates that the electrochemical oxidation reaction occurs efficiently, and a linear value indicates that the concentration is proportional to the Q value.

Photoelectrochemical response of synthetic samples.

Four types of organic compounds were selected as the analysis targets to evaluate the applicability of the proposed method: glucose, oxalic acid, benzoic acid, and potassium hydrogen phthalate (KHP). The photocurrent response at various concentrations of organic compounds is shown in Figure 9.

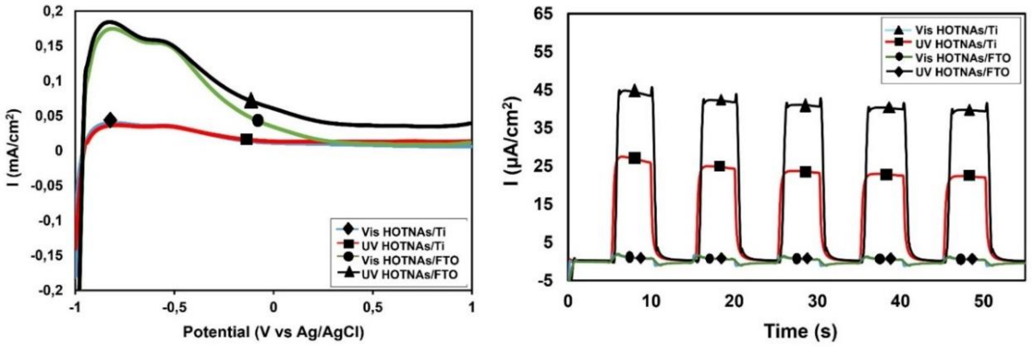

(a) (b)

Figure 7. Graph of electrochemical testing using (a) HOTNAs/Ti and HOTNAs/FTO using LSV, (b) HOTNAs/Ti and HOTNAs/FTO using MPA

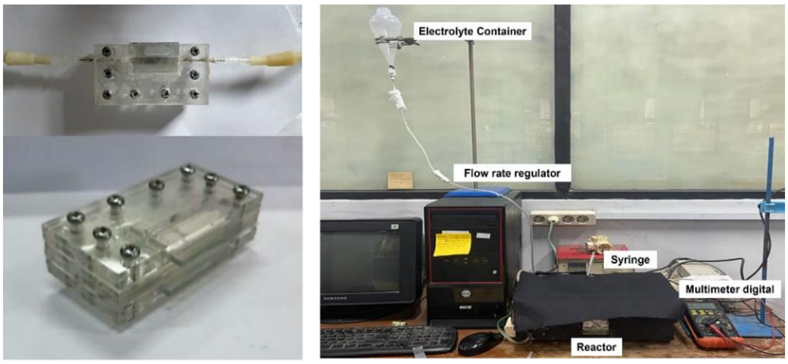

(a) (b)

Figure 8. (a) COD sensor probe, (b) the overall arrangement of the FIA system

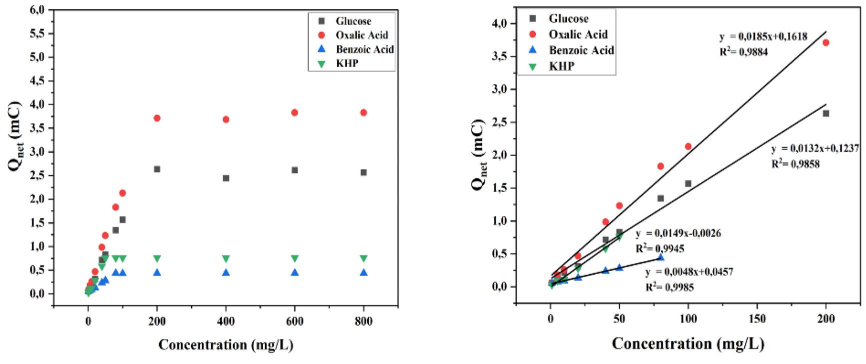

(a) (b)

Figure 9. (a) The trend of increasing the compound charge (Q_{net} with increasing concentration up to a concentration range of 800 mg/L, (b) The net charge linearity area (Q_{net})

The value of Q was obtained from Equation 2. In Figure 9 a, all these organic compounds show increased Q_{net} with increasing compound concentration. Figure 9 b shows that all those organic compounds show an excellent linear relationship to some extent. Glucose linearity is 1-200 mg/L, oxalic acid is 1-200, benzoic acid linearity is 1-80 mg/L, and KHP is 1-50mg/L. This limit indicates that the concentration of the compound in the sample has reached the maximum point that the photocatalyst on HOTNAs/FTO can oxidize (Nurdin *et al*. 2010).

Response of Current in Standard Addition Method to Samples.

The measurements using the standard addition method were carried out on a series of matrices containing the desired analyte without the addition of standard analytes or with the addition of standard analytes of known concentrations. Tests were carried out using the same organic substance with different organic substances and mixed compounds for samples and standard addition solutions.

The relationship between the charge value obtained from the measurement and the concentration of the standard addition solution is presented in Figure 10. Figure 10a is the linearity of the charge in the standard addition method for samples containing the same substance. This test is carried out to ensure that the method used can accurately measure compounds. The sample concentrations were glucose, oxalic acid, benzoic acid of 50 mg/L, and KHP concentration of 10 mg/L.

The calculated concentration at the time of measurement can be calculated through the linear equation for which the equation was measured:

$$C = \frac{a\ x\ V_t}{b\ x\ V_s} \quad \dots (11)$$

where c, a, b, Vt, and Vs. are sample concentration, slope, intercept, total volume, and sample volume, respectively.

According to equation 11, glucose, oxalic acid, benzoic acid, and KHP concentrations at measurement were 53.09 mg/L, 51.11 mg/L, 55.59 mg/L, and 11.99 mg/L, respectively. Figure 10b shows the linearity of the charge in the standard addition method for samples and standard addition solutions with different compounds. This test is carried out to ensure that the analysis can provide accurate and relevant results in the presence of a matrix or other compounds that may be present in the sample. According to equation 11, the concentrations of the glucose and KHP samples calculated during measurement were 50.87 mg/L and 12.04 mg/L. Figure 10c shows the linearity of the charge in the standard addition method with samples and standard addition solutions containing mixed solutions. This test assessed the response to the interaction between the sample and the complex matrix (Hasegawa *et al*. 2021; MacHovec 1980). Glucose was chosen as the standard addition solution because glucose has a wide area of linearity. The concentrations of the glucose samples and mixed solutions used were 50 mg/l and 200 mg/l, respectively. According to equation 11, the concentrations of glucose and mixed compounds are 57.78 mg/L and 203.5 mg/L. The %measurement error is obtained from these results, presented in Table 1. %Error is the percentage difference between the sample and measured concentrations.

COD Sensor Response to all Test Compounds.

The response of the test compound compared to the concentration (mg/L O_2) to charge (Q) is shown in Figure 11. Furthermore, the response of the test compound using standard addition compared to the concentration (mg/L O_2) to charge (Q) is shown in Figure 12. Figures 11 and 12 are derived from figures 9 and 10 by plotting Q_{net} against theoretical COD values. Figure 9 shows the linear relationship between Q_{net} and COD at 1 to 50 mg/L concentrations. The slope of the various compounds reveals the number of electrons captured based on equation 4, which are suitable for oxidizing one mol of organic compounds with n glucose, oxalic acid, benzoic acid, and KHP are 24, 2, 30, and 29. It is

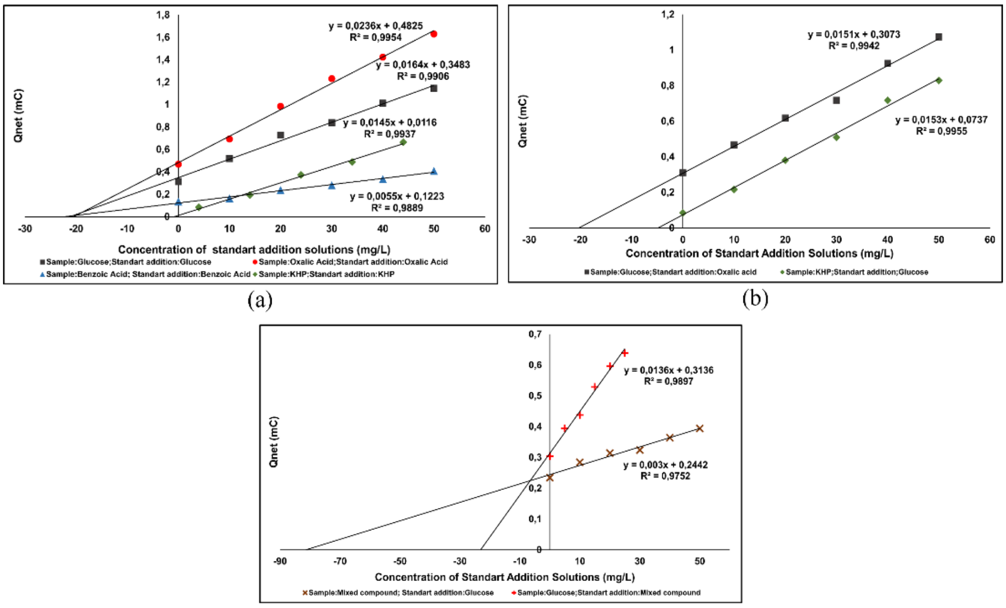

(a)

(b)

(c)

Figure 10. Linearity of the charge (Q_{net}) in the standard addition method to samples containing (a) the same substance, (b) different substances, and (c) mixed compounds

Table 1. Concentration determination results of various samples with various standard addition types measured by the proposed photoelectrochemical (PE) probe.

Sample	Standard addition solution	Designed sample concentration (mg/L)	The concentration of sample obtained by PE probe (mg/L)	%Error
Glucose	Glucose	50	53.09	6.19
Oxalic acid	Oxalic acid	50	51.11	2.22
Benzoic acid	Benzoic acid	50	55.59	11.18
KHP	KHP	10	11.99	19.99
Glucose	Oxalic acid	50	50.87	1.75
KHP	Glucose	10	12.04	20.42
Mixed solution	Glucose	200	203.5	1.75
Glucose	Mixed Solution	50	57.78	15.56

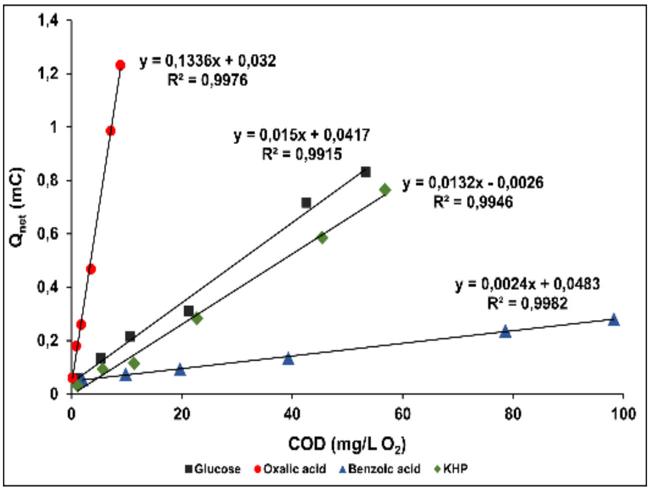

Figure 11. Response of the test compound compared to concentration (mg/L O_2) to charge (Q)

identical to theoretical order according to equation 3 (Li *et al.* 2008).

The effect of ions and molecules on the sample also results in slope differences. Figure 12a is the response of the test compound using standard addition using the same substance for the sample and standard addition solution. The sample consisted of glucose, oxalic acid, benzoic acid, and KHP samples with a COD value of 21.21 mg/L, 4.55 mg/L, 1.61 mg/L, and 45.1 mg/L O_2. Figure 12b is the response of the test compound using standard addition by using different substances for samples and standard addition solutions. Samples of glucose and KHP samples had a COD value of 21.28 mg/L and 5.11 mg/L O_2. Figure 12c is the response of the test compound with standard addition using mixed compounds for samples and standard addition solutions. Samples of glucose samples and mixed compounds had COD values of 25.08 mg/L and 87.21 mg/L O_2.

Real wastewater samples were analyzed using the proposed and conventional methods to demonstrate the feasibility of the device proposed in this study. The samples used were surface water from Danau Kenanga and Danau Agathis within the University of Indonesia Depok Campus and typical Laundry activity wastewater in the local area. The results are summarized in Table 2. The COD values determined

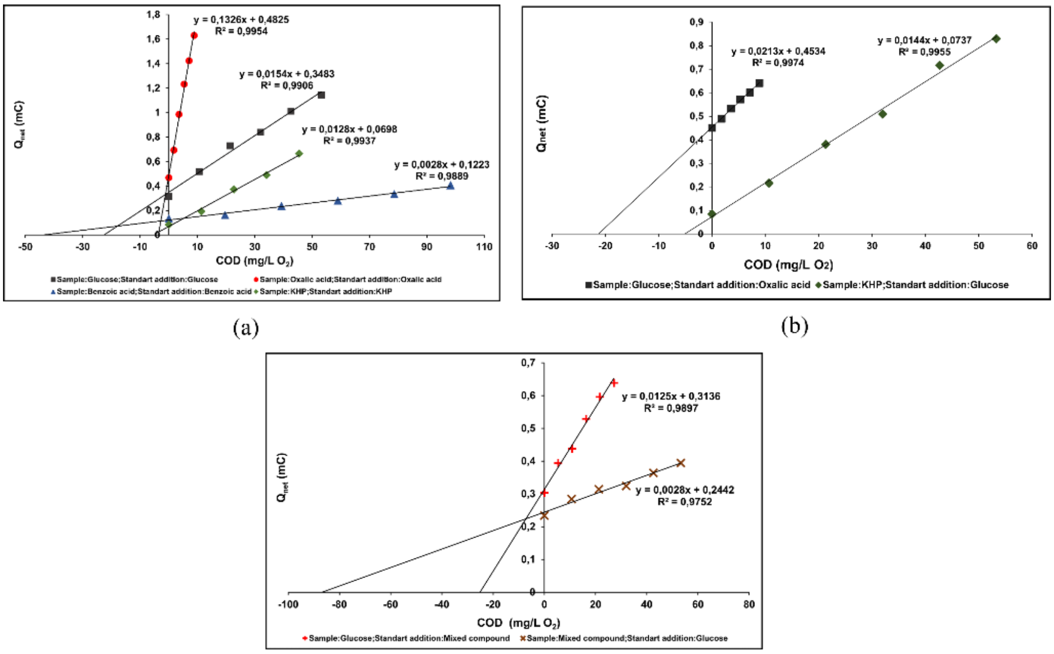

(a) (b)

(c)

Figure 12. Response of the test compound using standard addition by using (a) the same substance, (b) different substances, and (c) mixed compounds for samples and standard solutions compared to the concentration (mg/LO_2) to the charge (Q)

Table 2. Comparison of the results of environmental sample determination between the conventional dichromate standard method and the photo electrocatalytic chemical oxygen demand (PECOD) method

Sample	COD values measured by Conventional Dichromate Standard Method (mg/L O_2)	COD values measured by the PECOD method (mg/L O_2)	
		Measured with Glucose Standard Compounds	Measured with Mixed Compound Standards
Danau Kenanga surface water	14,95	15,4659 ± 0,1555 (%Error: 3,4514)	15,9571 ± 0,0616 (%Error: 6,73)
Danau Agathis surface water	18,7	19,05 ± 0,4216 (%Error: 1,8716)	19,6179 ± 0,5669 (%Error: 4,9088)
Typical Laundry wastewater	453,8	445,2336 ± 2,4662 (%Error: 1,924)	449,783 ± 0,7031 (%Error: 0,8931)

by the proposed sensor are in agreement with the conventional dichromate method, with a %error below 10%. The results of COD sensor measurements imply that the sensor can be used to measure COD concentrations in water samples with high accuracy. These sensors can be used for various applications, such as water quality monitoring, pollution control, and environmental research.

CONCLUSION

The photo-electrocatalytic chemical oxygen demand (PECOD) determination method was developed by employing HOTNAs/FTO photo-electrodes with the flow injection analysis system. Applying the PECOD method to measure synthetic and environmental samples has proved excellent. The results of environmental samples using the conventional dichromate method and the proposed PECOD are in agreement (within a 10% error). The proposed method is easy, simple, inexpensive, and no toxic reagents are involved.

ACKNOWLEDGMENT

The authors are grateful to the University of Indonesia and the TIPEC team (titania photo electro catalysis) for their support and enthusiasm for the research’s success.

REFERENCES

Abbas, W.A., Abdullah, I.H., Ali, B.A., Ahmed, N., Mohamed, A.M., Rezk, M.Y., Ismail, N., Mohamed, M.A. & Allam, N. K. (2019). Recent advances in the use of TiO2 nanotube powder in biological, environmental, and energy applications. *Nanoscale Advances*. **1(8)**: 2801–2816.

Alkorbi, A.S., Kumar, K.Y., Prashanth, M.K., Parashuram, L., Abate, A., Alharti, F.A., Jeon, B. & Raghu, M.S. (2022). Samarium vanadate affixed sulfur self doped g-C3N4 heterojunction; photocatalytic, photoelectrocatalytic hydrogen evolution and dye degradation. *International Journal of Hydrogen Energy*. **47(26)**: 12988-13003.

Azer, B. B., Gulsaran, A., Pennings, J.R., Saritas, R., Kocer, S., Bennett, J.L., Abhang, Y.D., Pope, M.A., Abdel-Rahman, E. & Yavuz, M. (2022). A Review: TiO_2 based photoelectrocatalytic chemical oxygen demand sensors and their usage in industrial applications. *Journal of Electroanalytical Chemistry*. **918**: 116466.

Cao, W., Chen, K. & Xue, D. (2021). Highly ordered TiO_2 nanotube arrays with engineered electrochemical energy storage performances. *Materials*. **14(3)**: 510.

Cazaudehore, G., Schraauwers, B., Peyrelasse, C., Lagnet, C. & Monlau, F. (2019). Determination of chemical oxygen demand of agricultural wastes by combining acid hydrolysis and commercial COD kit analysis. *Journal of Environmental Management*. **250**: 109464.

Chen, W., Liu, S., Fu, Y., Yan, H., Qin, L., Lai, C., Zhang, C., Ye, H., Chen, W., Qin, F., Xu, F., Huo, X. & Qin, H. (2022). Recent advances in photoelectrocatalysis for environmental applications: Sensing, pollutants removal and microbial inactivation. *Coordination Chemistry Reviews*. **454**: 214341.

Chougala, L.S., Yatnatti, M.S., Linganagoudar, R.K., Kamble, R.R., & Kadadevarmath, J.S. (2017). A simple approach on synthesis of TiO2 nanoparticles and its application in dye sensitized solar cells. *Journal of Nano- and Electronic Physics*. **9(4)**: 1–6.

Fu, Y., & Mo, A. (2018). A review on the electrochemically self-organized titania nanotube arrays: synthesis, modifications, and biomedical applications. *Nanoscale Research Letters*. **13**: 1-21.

Garcia-Segura, S., & Brillas, E. (2017). Applied photoelectrocatalysis on the degradation of organic pollutants in wastewaters. *Journal of Photochemistry and Photobiology C: Photochemistry Reviews*. **31**: 1-35.

Hasegawa, K., Minakata, K., Suzuki, M. & Suzuki, O. (2021). The standard addition method and its validation in forensic toxicology. *Forensic Toxicology*. **39(2)**: 311-333.

He, G., Wang, X., Xi, M., Zheng, F., Zhu, Z. & Fong, H. (2013). Fabrication and evaluation of dye-sensitized solar cells with photoanodes based on electrospun TiO_2 nanotubes. *Materials Letters*. **106**: 115-118.

Kangkun, N. & Ponchio, C. (2020). Photoelectrodeposition of BiVO4 layer on FTO/WO3 photoanodes for highly efficient photoelectrocatalytic chemical oxygen demand sensor applications. *Applied Surface Science*. **526**: 146686.

Li, M., Xiao, X. & Liu, R. (2008). Synthesis and bioactivity of highly ordered TiO_2 nanotube arrays. *Applied Surface Science*. **255(2)**: 365-367.

MacHovec, F. (1980). A systematic approach to standard addition method in instrumental analysis. *Journal of Chemical Education*. **57(10)**: 703-706.

Misriyani, M., Wahab, A. W., Taba, P. & Gunlazuardi, J. (2015). Application of TiO_2 Nanotube as Photoelectrode For Corrosion Prevention of Stainless Steel In pH Variation of NaCl. *Indonesian Journal of Chemical Research*. **3(1)**: 242-248.

Nogueira, R.P., Uchoa, J.D., Hilario, F., Santana-Melo, G.D.F., De Vasconcellos, L.M.R., Marciano, F.R., Roche, V., Moreira Jorge Junior, A. & Lobo, A.O. (2021). Characterization of optimized Ti_{O2} nanotubes morphology for medical implants: Biological activity and corrosion resistance. *International Journal of Nanomedicine*. **16**: 667–682.

Nurdin, M., Wibowo, W., Surahman, H., Krisnandi, Y. K. & Gunlazuardi, J. (2009). Pengembangan metode baru penentuan chemical oxygen demand (COD) berbasis sel fotoelektrokimia: karakterisasi elektroda kerja lapis tipis TiO_2/ITO. *Makara Journal of Science*. **13(1)**: 1-8.

Ocampo, R.A., Bedoya Ochoa, N., Tamayo, J.A., Botero, C., Vargas, C.A., Gómez, M., Castaño, J.G. & Zuleta Gil, A.A. (2023). Formation of highly ordered TiO_2 nanotubes on Ti6Al4V alloys manufactured by electron beam powder bed fusion (E-PBF). *The International Journal of Advanced Manufacturing Technology*. **128(1-2)**: 257-266.

Puga, M.L., Venturini, J., Ten Caten, C.S. & Bergmann, C. P. (2022). Influencing parameters in the electrochemical anodization of TiO_2 nanotubes: Systematic review and meta-analysis. *Ceramics International*. **48(14)**: 19513-19526.

Si, H., Pan, N., Zhang, X., Liao, J., Rumyantseva, M. N., Gaskov, A.M. & Lin, S. (2019). A real-time on-line photoelectrochemical sensor toward chemical oxygen demand determination based on field-effect transistor using an extended gate with 3D TiO_2 nanotube arrays. *Sensors and Actuators B: Chemical*. **289**: 106-113.

Singh, R., Majumder, C.B. & Vidyarthi, A.K. (2023). Assessing the impacts of industrial wastewater on the inland surface water quality: An application of analytic hierarchy process (AHP) model-based water quality index and GIS techniques. *Physics and Chemistry of the Earth, Parts A/B/C*. **129**: 103314.

Syauqi, M. I., Prasetia, P., & Gunlazuardi, J. (2023). The influence of sodium alginate in water-based electrolyte on the morphology of TiO_2 nanotube prepared by anodization method. *Materials Chemistry and Physics*. **296**: 127234.

Syeed, M.M., Hossain, M.S., Karim, M.R., Uddin, M.F., Hasan, M. & Khan, R. H. (2023). Surface water quality profiling using the water quality index, pollution index and statistical methods: A critical review. *Environmental and Sustainability Indicators*. **18**: 100247.

Tesler, A. B., Altomare, M. & Schmuki, P. (2020). Morphology and optical properties of highly ordered TiO_2 nanotubes grown in NH_4F/o-H_3PO4 electrolytes in view of light-harvesting and catalytic applications. *ACS Applied Nano Materials*. **3(11)**: 10646-10658.

Yang, P., Liu, Y., Chen, S., Ma, J., Gong, J., Zhang, T. & Zhu, X. (2016). Influence of H_2O_2 and H2O content on anodizing current and morphology evolution of anodic TiO2 nanotubes. *Materials Research Bulletin*. **83**: 581-589.

Yu, J., Yu, H., Cheng, B. & Trapalis, C. (2006). Effects of calcination temperature on the microstructures and photocatalytic activity of titanate nanotubes. *Journal of Molecular Catalysis A: Chemical*. **249(1-2)**: 135-142.

Žerjav, G., Žižek, K., Zavašnik, J. & Pintar, A. (2022). Brookite vs. rutile vs. anatase: Whats behind their various photocatalytic activities?. *Journal of Environmental Chemical Engineering*. **10(3)**: 107722.

Zhang, S., Zhao, H., Jiang, D. & John, R. (2004). Photoelectrochemical determination of chemical oxygen demand based on an exhaustive degradation model in a thin-layer cell. *Analytica Chimica Acta*. **514(1)**: 89-97.

Zhao, H., Jiang, D., Zhang, S., Catterall, K. & John, R. (2004). Development of a direct photoelectrochemical method for determination of chemical oxygen demand. *Analytical Chemistry*. **76(1)**: 155-160.